STSM REPORT

COST STSM Reference Number: ECOST-STSM-BM1205-150217-082209

STSM Applicant: Aleksandar Demić

STSM Topic: Laser imaging methods for biomedical applications: optical feedback imaging with terahertz quantum-cascade lase

Home Institution: School of Electronic and Electrical Engineering, University of Leeds, Leeds (UK)

Host Institution: School of Information Technology and Electrical Engineering, University of Queensland, Brisbane (Australia)

STSM period: 26/02/2017 to 17/03/2017

COST Action: BM1205

STSM purpose: The goal of this short term scientific mission is for the applicant to broaden knowledge in self-mixing interferometry in terahertz (THz) quantum cascade lasers (QCLs), and boost collaboration with the host, on the subject of application of this technology in medical imaging and chemical sensing. The applicant is designing a fully dynamic model for QCLs as part of his PhD thesis. At the moment, models for QCL physics under feedback are only capable of modeling steady - state operation without coherent transport contribution, while the applicant's model promises ability to model full coherent QCL dynamics under feedback as first of its kind, on the other hand host's group represents the leading experimental group for self-mixing interferometry, thus this visit will be beneficial to both ends. The visit will focus on the further refinement of the model with the final aim to design THz QCL heterostructures for validating experimental results and to propose novel structures which are expected to give optimal performance useful for imaging and sensing applications. After the mission is completed it is envisioned that upon experimental confirmation of optimized structures we would have optimized set-up for the particular imaging/sensing application.

Description of the main results obtained:

1. Introduction

Bound-to-continuum (BTC) THz QCL structure is commonly used in applications where reasonably low threshold current is needed in order to achieve continuous-wave (CW) operation. BTC QCL has large number of quantum well and barrier layers in one active region period and corresponds to substantial number of quantum-confined subbands involved in electron transport, therefore development of proper theoretical model for electron transport in it is a challenging task.

Two models have been developed in School of Electronic and Electrical Engineering at University of Leeds so far. Full rate equation (RE) approach, where all relevant electron states are considered, and used to derive detaile information about the intersubband transitions, with the dependencies of scattering processes upon lattice temperature and external bias (terminal voltage) in semi-classical treatment. Density matrix approach (DM), where transport within the QCL device is treated through quantum mechanics and this provides more reliable results then RE.

Main shortcoming of RE model is the inability to describe coherent effects in QCL which in simulation results in formation of unphysical spikes in current density, material gain and state populations profile. On the other hand DM model yields smooth output profiles and shows promise for various applications.

Self-mixing interferometry (SM) needs to take into account the light that returns to the laser cavity after a reflection on the target [1]. This results in terminal voltage oscillations which hold the information of target's properties, thus it is possible to obtain source and the detector within the same device. Physical modeling of this effect is treated through Lang-Kobayashi model [2] and the only model that currently exists in the literature for QCLs is Reduced Rate Equation (RRE) model [3], developed by the School of Information Technology and Electrical Engineering, University of Queensland, Brisbane (Australia). This model focuses on two states in the QCL period that perform the lasing and it is naturally coupled with the full RE approach from which it needs input information. The main difficulty during the modeling is highly non-linear data with presence of high number of unphysical points. This issue was addressed through manual removal of unwanted data and polynomial fitting procedures in order for RRE model to provide sensible set of the results. Such modeling technique naturally holds the possibility of losing some physical effects in the model and it also raises the need for extensive input data processing.

During this STSM, RRE model was improved by generating the input data from DM model and formation of unphysical spikes and a need for their removal and polynomial fitting was completely avoided.

2. Density matrix model

Density matrix model is formulated through consideration of the transport within the nearest neighbor approximation. Central QCL period (CC) interacts with upstream period (UU) and downstream period (DD), interactions within the CC, UU and DD periods are treated in semi-classical manner (through Fermi's golden rule) which is the case in RE model as well, but interperiod transport is treated in coherent quantum mechanical manner where it is assumed that under resonant condition, transport through the injection barrier is not instantaneous and it can be described through oscillation at Rabi's frequency. It should be noted that this 3 period structure contains the periodic symmetry of QCL device and that interaction between UU and CC periods will be the same as interaction between CC and DD periods, and vice versa. Implementing this symmetry beforehand results in the Hamiltonian and density matrix of the form:

$$H = \begin{bmatrix} H_{UU} & H_{UC} & 0 \\ H_{CU} & H_{CC} & H_{UC} \\ 0 & H_{CU} & H_{DD} \end{bmatrix}, \ \rho = \begin{bmatrix} \rho_{CC} & \rho_{UC} & 0 \\ \rho_{CU} & \rho_{CC} & \rho_{UC} \\ 0 & \rho_{CU} & \rho_{CC} \end{bmatrix}$$
$$H_{CC} = \begin{bmatrix} E_3 & 0 & 0 \\ 0 & E_2 & 0 \\ 0 & 0 & E_1 \end{bmatrix} + eZ\,E(t) \ , H_{UC} = \begin{bmatrix} \Omega_{3U-3} & \Omega_{3U-2} & \Omega_{3U-1} \\ \Omega_{2U-3} & \Omega_{2U-2} & \Omega_{2U-1} \\ \Omega_{1U-3} & \Omega_{1U-2} & \Omega_{1U-1} \end{bmatrix} \quad (1)$$

in which the block subscripts describe interaction terms between the central (C), upper (U) and lower (D) periods. The off-diagonal elements correspond to the coupling between the periods labeled by the corresponding indices. It also applies $H_{UU} = H_{CC} + eKL, \quad H_{DD} = H_{CC} - eKL$ where K is the applied external bias, and L is the length of the single QCL period. Central period Hamiltonian consists of single module tight binding energies on the main diagonal and optical field interaction is added through dipole approximation where Z is dipole matrix and $E(t)$ is optical electric field. It applies that $H_{UC} = (H_{CU})^T$ and this matrix is filled with Rabi coupling terms, calculated as in [4]. In (1) H_{CC} and H_{UC} are given for the case when 3 states are considered within the period. The model is extendable to arbitrary number of states in the module.

Scattering processes are added in the form ρ/τ and overall matrix form looks similar to H and ρ. Full discussion on this model can be found in [5,6,7]. Transport process in DM is presented in Fig. 1.

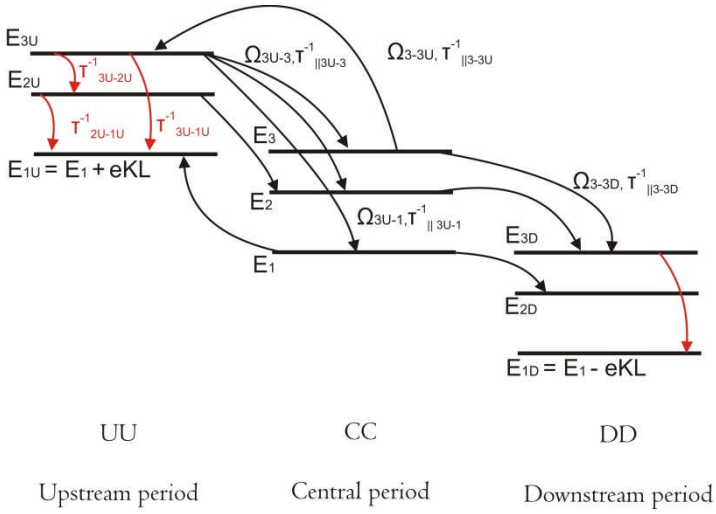

Figure 1. Phenomenological illustration of DM model and interactions that occur. Intraperiod scattering (red arrows) is treated in semi-classical approach, while interperiod transport (black arrows) is treated as coherent tunnelling with Rabi coupling Ω_{ij} energy and dephasing time $\tau_{||_{ij}}$.

The Hamiltonian, corresponding density matrix and scattering matrix are all substituted in the equation of motion (Liouville equation):

$$\frac{d\rho}{dt} = -\frac{i}{\hbar}[H,\rho] - \left(\frac{\rho}{\tau}\right)_{relax} \quad (2)$$

Note that substitution of 3-period Hamiltonian and density matrix into (2) does not fully implement periodic boundary conditions of the system (even though we implemented the symmetry of the system beforehand). In order to formulate the nearest neighbor approximation, infinite Hamiltonian structure and density matrix needs to be substituted into the Liouville equation, and this needs to be considered in the derivation of the output from the model as presented in [7].

Equation of motion therefor breaks down to the system [7]:

$$\frac{d}{dt}\begin{bmatrix}\rho_1 \\ \rho_2 \\ \rho_3\end{bmatrix} = -\frac{i}{\hbar}\begin{bmatrix}[H_1,\rho_1] + [H_2,\rho_3] + [H_3,\rho_2] \\ [H_2,\rho_1] + H_{1U}\rho_2 - \rho_2 H_1 \\ [H_3,\rho_1] + H_1\rho_3 - \rho_3 H_{1U}\end{bmatrix} - \begin{bmatrix}\rho_1/\tau \\ \rho_2/\,\tau \\ \rho_3/\tau\end{bmatrix} \quad (3)$$

where we switched to numerical indices (CC = 1, UC = 2 and CU = 3). This system has 3 unknown matrices, each with N^2 unknown elements (where N is the number of considered states in the single QCL module). Since the unknown matrices are part of commutators, direct linearization is not possible. Mathematical approach to write this system in linear form is to linearize each commutator in the system separately. Mathematically, this is performed through Kronecker tensor product $\otimes$, and a commutator $[H_i, \rho_i] \rightarrow L_i \rho_i'$ linearizes as $L_i = H_i \otimes I - I \otimes H_i^T$ where ρ_i' is column vector of N^2 elements which are taken row-wise from the original unknown ρ_i matrix and L_i is the system matrix of $N^2 \times N^2$ size.

We can avoid time domain solution of this system by non-rotating wave approximation (nRWA) where each unknown in the system is assumed to have 3 harmonics: $\rho_i = \rho_i^{DC} + \rho_i^{+} e^{iwt} + \rho_i^{-} e^{-iwt}$, and $H_i = H_i^{DC} + H_i^{+} e^{iwt} + H_i^{-} e^{-iwt}$, for $i = 1,2,3$. Central block is the only block that has AC parts and this simplifies the overall system. This approximation causes (3) to expand to $9N^2 \times 9N^2$ system. Even though the system is extensive, its numerical implementation is more efficient than RE and provides the ability for generalization of the model for multi-mode operation or self-mixing.

Current density is calculated as $j = \lim_{Q \to \infty} \frac{1}{Q} \frac{ien_{2D}}{\hbar L} Tr(\rho[H, Z_{total}])$, where H is full (infinite period Hamiltonian with $Q \to \infty$ periods) and Z_{total} is corresponding dipole matrix for the entire structure. Material gain is extracted from current density by considering harmonic response of the DM terms to a light field $E(t) = A_0 e^{iwt}$ and this is calculated as $-Im\{\varepsilon\} v_g / w$ where v_g is group velocity, and ε is the complex permittivity of electron gas which is calculated as $j^+ / \frac{dE}{dt}$ where j^+ is AC part of current density. The main expressions for DM output are:

$$\begin{aligned} j_{DC} &= -\frac{ien_{2D}}{\hbar L} Tr\left(Z([H_1^{DC}, \rho_1^{DC}] + [H_1^{AC}, \rho_1^{+} + \rho_1^{-}] + [H_2, \rho_3^{DC}] + [H_3, \rho_2^{DC}]) + L(H_2 \rho_3^{DC} - \rho_2^{DC} H_3)\right) \\ g &= \frac{en_{2D}}{n_r c \varepsilon_0 \hbar A_0 L} Im\left\{Tr\left(Z([H_1^{DC}, \rho_1^{+}] + [H_1^{AC}, \rho_1^{DC}] + [H_2, \rho_3^{+}] + [H_3, \rho_2^{+}])\right)\right\} \end{aligned} \quad (4)$$

Terms in (4) for j_{DC} calculation are also present in the first equation of the system in (3) and j_{DC} can be therefor represented through the scattering part of (4), it can be shown that:

$$j_{DC} = \frac{e}{L}\left(\sum_i \sum_{j \neq i} n_i \left(\frac{Z_{ii} - Z_{jj}}{\tau_{ij}}\right) + \sum_i \sum_{j \neq i} Z_{ij} \frac{n_{2D} \rho_1^{DC}{}_{ji}}{\tau_{||ji}}\right) + \frac{ien_{2D}}{\hbar} Tr(H_2 \rho_3^{DC} - \rho_2^{DC} H_3) \quad (5)$$

The first term in (5) represents the expression for calculation of current in RE approach, the difference from DM lies in the fact that in RE τ_{ij} represents all scattering rates in the systems, both interperiod and intraperiod, while in DM τ_{ij} are only intraperiod scattering rates, while interperiod transport is treated through Rabi coupling strengths (contained in $H_{2/3}$) and dephasing times, as depicted in Fig. 1.

3. Numerical results

In this STSM, analyzed BTC QCL structure is designed for 2 THz emission and based on design presented in [8]. Fig. 1 shows the band structure diagram, calculated using the full self-consistent Schrödinger–Poisson energy balance scattering transport method [9,10].

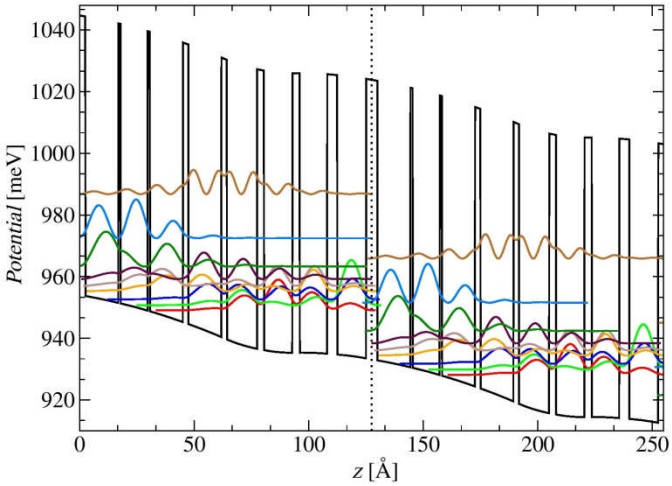

Figure 2. Layer thicknesses for analysing BTC QCL design, starting from the injection barrier (until dotted horizontal line), are **4.8**/15.03/**1.0**/11.54/**0.99**/13.82/**2.3**/14.53/**2.5**/*12.54*/**2.9**/*11.78*/**3.0**/11.4/**4.2**/11.97 $Al_{0.1}Ga_{0.9}As$ barriers are shown in bold and wells doped at 1.3 10^{16} cm^{-3} are underlined. Two periods are presented along with corresponding wavefunctions, applied electric field is 1.64 kV/cm.

In our modeling procedure we use 3 fitting parameters in order to compare our results with the experimental data: total loss in the laser cavity, interface roughness (IFR) scattering parameters and contact resistance.

Cavity loss directly determines the lasing threshold and this can be estimated by various waveguide models. In this work we use 1-dimensional transfer matrix calculation of waveguide modes, with Drude-Lorentz model for permittivities, as described in [11].

The IFR parameters are not experimentally known, and can vary from structure to structure. This brings the need for additional sweeping of these parameters in the simulation and the optimal values depend on the fitting goals: obtaining threshold fit, peak power fit or roll over fit (ideally the entire *I-V* and *L-I* fit).

Contact resistance parameter can significantly shift *I-V* characteristics and approximate values can be obtained experimentally. Typical values are several Ohms [12].

For the device in Fig 2. we used model from [11] to estimate the losses to 32.42 cm^{-1} in pulsed operation at cold finger temperature of 20 K. The design in Fig. 2 has the experimental dynamic range of 0.837 - 1.08 A and IFR parameters are found to match threshold current assuming a cavity loss of 32.42 cm^{-1}, this is illustrated in Fig. 3. Then we search for the value of contact resistance that fits the experimental data, this is estimated to 2.15 Ω.

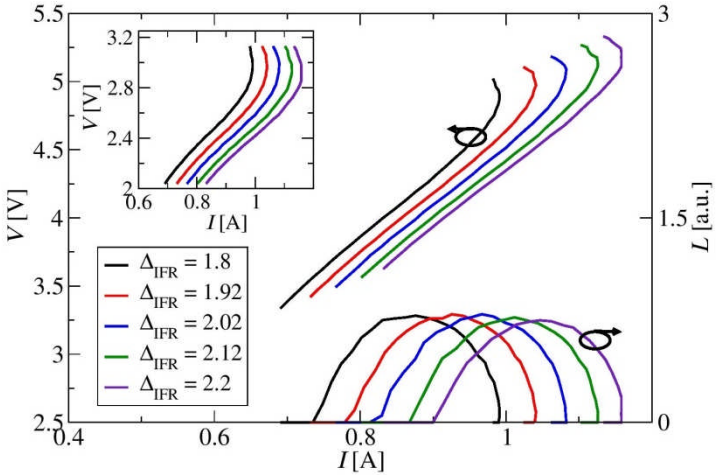

Figure 3. Density matrix model *I-V* characteristics for various values of interface roughness height Δ_{IFR} interface roughness correlation length was set to $\lambda = 80\,\dot{A}$. Contact resistance of 2.15 Ω is also included. Inset shows the *I-V* results without the contact resistance. *L-I* results are also presented for every Δ_{IFR} accordingly and normalized to unit value.

Figure 3 shows that $\Delta_{IFR} = 2.02\,\dot{A}$ gives the desired dynamic range for DM model. Interestingly, this value will not be the same in RE model due to the differences in intraperiod transport. RE fitting procedure relies only on fitting the threshold point. We found that the lasing threshold will occur for $K = 1.64\ kV/cm$ in both approaches. Gain spectrum and current density profile is presented in Fig. 4.

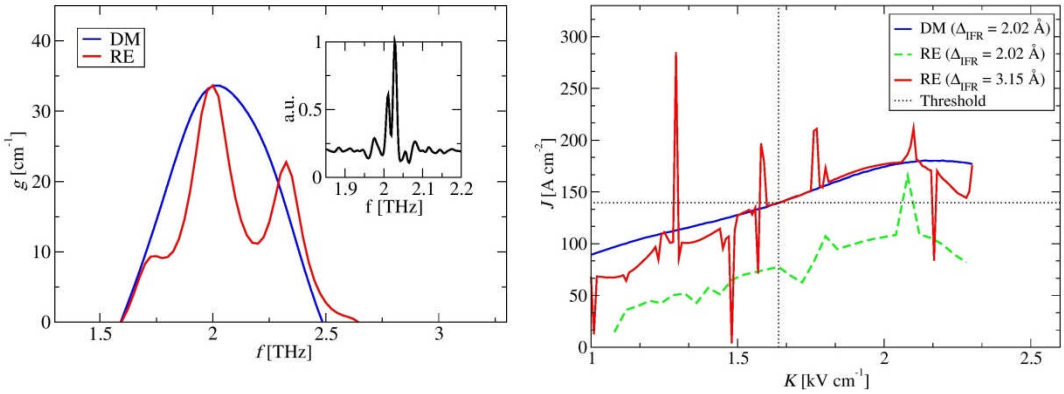

Figure 4. **a)** Gain versus frequency at lasing threshold point - the graph shows that lasing emission is expected around 2.06 THz. **b)** Current density versus bias. DM results are colored blue, while RE are colored red. The green dashed line represents the RE simulation under same condition as in the DM model and this clearly illustrates the need for different fitting procedure then in DM.

Current-voltage (*I-V*) characteristic of the device is obtained from Fig. 4b) by scaling the results with corresponding device dimensions and this is illustrated in Fig. 5.

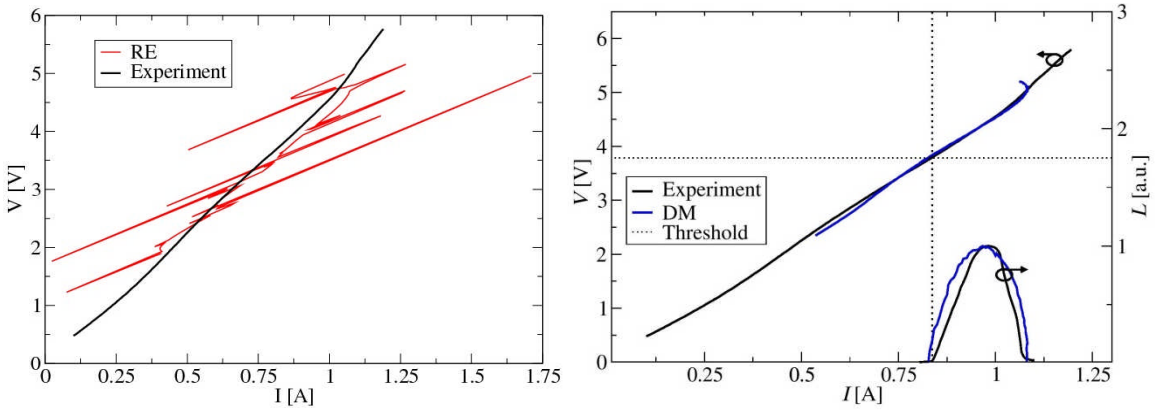

Figure 5. a) *I-V* characteristic from RE model. **b)** *I-V* characteristic from DM model along with normalized *L-I* characteristic depicting the dynamic range. Contact resistance of 2.15 Ω is used in both approaches.

The result in Fig. 5 shows the greatest advantage of DM model which provides smooth results that compare very well with the experimental data and shows good promise for RRE model input. The main shortcoming of DM (and RE) model is the inability to model continuous wave operation of QCL. At the moment, both models assume that lattice temperature equals to the cold finger temperature which is only true for pulsed operation at low temperatures. Since IFR parameters do not depend on temperature we can observe DM results under higher cold finger temperatures and compare dynamic ranges with the experimental ones. This is illustrated in Fig. 6.

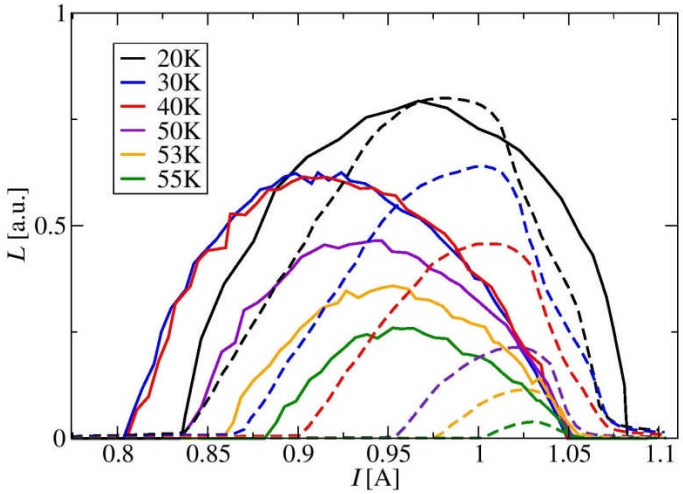

Figure 6. *L-I* characteristics for different cold finger temperatures. Full lines represent simulation result, while dashed lines represent the experimental measurement. Scaling was performed so peak ratio is consistent in both results.

Figure 6 provides comparison of *L-I* data for different temperatures. We can notice that the model gives similar dynamic ranges at 20, 30 and 40 K, and that the sharp drop of peak power is only noticeable at higher temperatures. Such behavior is related to exponential drop of the upper lasing level state lifetime with temperature in BTC structures [13] which becomes significant in the similar temperature range as in Fig. 6. It can also be noted that at higher temperatures the relative rate of theoretical power peaks match the experimental ones. The main reason for the mismatch of theoretical and experimental threshold current may be attributed to the lack of full thermal model within these calculations, which assume that heat sink temperature equals the lattice temperature in the device.

The overheating is certainly larger in CW operation, and the sensitivity of the gain on temperature is larger at higher temperatures, implying that the discrepancy between theoretical and experimental results will then be larger as well. Interestingly, dynamic range at cold finger temperature of 20K for CW operation is 0.971-1.1 A which matches the case of 53K in Fig 6 and this gives an idea about the overheating.

4. Mutual benefits for the Home and Host institutions

Collaboration with the host institution, School of Information Technology and Electrical Engineering, University of Queensland, Brisbane, Australia was very useful and stimulating. DM model shows great promise for future improvements of RRE model. RRE model needs input that depends on the applied bias and temperature. As illustrated, temperature effects in DM model still do not match experimental results and further development of this model will be benefit both institutions in the future.

Acknowledgment

I would like to express gratitude to Dr. Gary Agnew and Dr. Xiaoquiong Qi on explanations and discussions regarding RRE model. My sincere thanks also go to Dr Yah Lim, Dr Carl Bertling and Mr. She Han for experimental support and explanations on experimental procedure and theoretical modeling support that is required for the study of the measured data. Finally I'd like to thank the host Prof. Aleksandar Rakić on his support, discussions and guidance during the visit.

References

[1] T. Taimre, M. Nikolić, K. Bertling, Y. Lim, T.Bosch and A. Rakić, "Laser feedback interferometry: a tutorial on the self-mixing effect for coherent sensing", Advances in Optics and Photonics 7, 570 (2015).

[2] R. Lang and K. Kobayashi, "External optical feedback effects on semiconductor injection laser properties" IEEE J. Quant. Electron. QE-16, 347 (1980).

[3] G. Agnew, A. Grier, T. Taimre, Y. Lim, M. Nikolić, A. Valavanis, J. Cooper, P. Dean, S. Khanna, M. Lachab, E. Linfield, A. Davies, P. Harrison, Z. Ikonić, D. Indjin, and A. Rakić, "Efficient prediction of terahertz quantum cascade laser dynamics from steady-state simulations", Citation: Appl. Phys. Lett. 106, 161105 (2015).

[4] A. Yariv, C. Lindsey, and U. Sivan, "Approximate analytic solution for electronic wave functions and energies in coupled quantum wells," J.Appl. Phys., vol. 58, no. 9, pp. 3669–3672 (1985).

[5] T. V. Dinh, A. Valavanis, L. J. M. Lever, Z. Ikonic, and R. W. Kelsall, "Extended density-matrix model applied to silicon-based terahertz quantum cascade lasers," Phys. Rev. B, vol. 85, no. 23, p. 235427 (2012).

[6] A. Grier, P. Dean, A. Valavanis, J. Keeley, I. Kundu, J. D. Cooper, G. Agnew, T. Taimre, Y. L. Lim, K. Bertling, A. D. Rakic, L. H. Li, P. Harrison, E. H. Linfield, Z. Ikonic, A. G. Davies, and D. Indjin, "Origin of terminal voltage variations due to self-mixing in terahertz frequency quantum cascade lasers," Opt. Express, vol. 24, no. 19, pp. 21948–21956 (2016).

[7] A. Demić, A. Grier, Z. Ikonić, A. Valavanis, C. Evans, R. Mohandas, L. Li, E. Linfield, A. Davies and D. Indjin, "Infinite period density-matrix model for terahertz quantum cascade lasers", IEEE Transactions on Terahertz Science and Technology, *accepted for publication* (2017).

[8] J. Freeman, O. Marshall, H. Beere, and D. Ritchie, "Improved wall plug efficiency of a 1.9 THz quantum cascade laser by an automated design approach", Appl. Phys. Lett. 93, 191119 (2008).

[9] V. Jovanovic , D. Indjin, N. Vukmirovic , Z. Ikonic , P. Harrison, E. Linfield, H. Page, X. Marcadet, C. Sirtori, C. Worrall, H. Beere, and D. Ritchie, "Mechanisms of dynamic range limitations in GaAs/AlGaAs quantum-cascade lasers: Influence of injector doping," Appl. Phys. Lett. 86, 211117 (2005).

[10] J. Cooper, A. Valavanis, Z. Ikonic, P. Harrison, and J. Cunningham, "Finite difference method for solving the schrödinger equation with band nonparabolicity in mid- infrared quantum cascade lasers," J. Appl. Phys. 108, 113109 (2010).

[11] C. Evans, D. Indjin, Z. Ikonic, P. Harrison, M. S. Vitiello, V. Spagnolo, and G. Scamarcio, "Thermal modeling of terahertz quantum cascade lasers: Comparison of optical waveguides," IEEE Journal of Quantum Electronics, vol. 44, pp. 680–685, (2008).

[12] A. Grier, A. Valavanis, C. Edmunds, J. Shao, J. D. Cooper, G. Gardner, M. Manfra, O. Malis, D. Indjin, Z. Ikonić, and P. Harrison, "Coherent vertical electron transport and interface roughness effects in AlGaN/GaN intersubband devices," J. Appl. Phys., vol. 118, no. 22, p. 224308 (2015).

[13] D. Indjin, P. Harrison, R. W. Kelsall, and Z. Ikonic, "Mechanisms of temperature performance degradation in terahertz quantum-cascade lasers," Appl. Phys. Lett., vol. 82, no. 9, pp. 1347–1349 (2003).

STSM outcome form

STSM application number	Home Institution & country	Host institution & country	BM1205 WG	Objective of the collaboration	Results of the collaboration
ECOST-STSM-BM1205-150217-082209	School of Electronic and Electrical Engineering, University of Leeds, Leeds (UK)	School of Information Technology and Electrical Engineering, University of Queensland, Brisbane (Australia)	WG2/WG3	Self-mixing interferometry understanding and providing input for reduced rate equation model from density matrix model	- detail understanding of DM model - development of the code which automatically extracts the required input from DM model

THE UNIVERSITY OF QUEENSLAND
AUSTRALIA

School of Information Technology and Electrical Engineering

Professor Aleksandar Rakic

The University of Queensland
Brisbane Qld 4072 Australia
Telephone +61 7 3365 2097
Facsimile +61 7 3365 4999
Email enquiries@itee.uq.edu.au
Internet www.itee.uq.edu.au
CRICOS PROVIDER NUMBER 00025B

11 May 2017

To: BM1205 COST Action Chair and STSM Coordinator,

Dear Colleagues,

It is a pleasure to confirm that the School of Information Technology and Electrical Engineering within the University of Queensland, Brisbane hosted research visit of Mr Aleksandar Demic, from School of Electronic and Electrical Engineering, University of Leeds, UK. Aleksandar has successfully carried out research described in his BM1205 Short Term Scientific Mission (STSM) application. The focus of the research was in the field of laser feedback interferometry for imaging and material identification. In particular, as described in his STSM application, Aleksandar has been working on modelling the electron transport in terahertz (THz) quantum-cascade lasers, which will be used as an integrated source and detector in the imaging systems based on self-mixing effect. He has been collaborating with our Photonics and Microwave Engineering research group. This group has pioneered the development of several world's first laser-feedback interferometric sensors, including systems based on monolithic vertical-cavity surface-emitting laser arrays, blue-green lasers, terahertz quantum cascade lasers, and mid-infrared interband cascade lasers. The current focus of the group is on the development of sensing and imaging systems that exploit the THz spectrum for applications in vivo biomedical imaging.
We are confident that realized research activity is mutually beneficial for both Brisbane and Leeds research teams, would produce more joint publications, contribute strongly to results and impact of Aleksandar's PhD project and further strengthen research collaboration between our institutions.

Yours sincerely,

Professor Aleksandar Rakic
School Information Technology and Electrical Engineering
The University of Queensland, Brisbane, Australia